

Phonon-activated electron-stimulated desorption of halogens from Si(100)-(2×1)

B. R. Trenhaile, V. N. Antonov,* G. J. Xu,† Abhishek Agrawal, A. W. Signor, R. E. Butera, Koji S. Nakayama,‡ and J. H. Weaver

Department of Physics, Department of Materials Science and Engineering, and Frederick Seitz Materials Research Laboratory, University of Illinois at Urbana-Champaign, Urbana, Illinois 61801, USA

(Received 12 May 2005; revised manuscript received 11 January 2006; published 15 March 2006)

Spontaneous desorption of Cl, Br, and I from *n*- and *p*-type Si(100)-(2×1) was studied with scanning tunneling microscopy at temperatures of 620–800 K where conventional thermal bond breaking should be negligible. The activation energies and prefactors determined from Arrhenius plots indicate a novel reaction pathway that is initiated by the capture of electrons which have been excited by phonon processes into Si-halogen antibonding states. This configuration is on a repulsive potential energy surface, and it is sufficiently long lived that desorption can occur, constituting phonon-activated electron-stimulated desorption. Surprisingly, the Arrhenius plots for differently doped samples crossed and, above a critical temperature, the reaction with the largest activation energy had the highest rate. This is explained by large entropy changes associated with the multiphonon nature of the electronic excitation. For Cl desorption from *p*-type Si, these entropy changes amounted to $34k_B$. They were $19k_B$, $13k_B$, and $8k_B$ for Br desorption from *p*-type, lightly doped *n*-type, and heavily doped *n*-type Si, respectively. The desorption rates for I were nearly three orders of magnitude larger than the rates observed for Cl and Br. Here, the Si-I antibonding states overlap the conduction-band minimum, so that conduction-band electrons with this energy can be captured by the Si-I antibonding states. Together, these results reveal that a complex relationship exists between phonons and electronic excitations during chemical reactions at surfaces.

DOI: [10.1103/PhysRevB.73.125318](https://doi.org/10.1103/PhysRevB.73.125318)

PACS number(s): 68.37.Ef, 68.43.Mn, 68.43.Rs, 68.43.Vx

I. INTRODUCTION

Si(100) provides an ideal surface to study fundamental surface processes because of its relative simplicity and its rich literature. Generally, these surface processes have been split into two distinct camps depending on whether they were stimulated by electrons or photons or whether they were thermally activated. Electron- or photon-stimulated processes involve excited electronic states that obtained their energy from electrons or photons from an outside source (or secondary electrons following primary absorption).^{1,2} These processes result in the desorption of adatoms or the creation of defects.^{3–7} On the other hand, thermally activated processes such as diffusion, desorption, and etching are explained in terms of bond strengths, vibrational excitations, and potential energy surfaces while largely ignoring the role of entropy and the effects of excited electronic states.^{8–11} The assumed separability of lattice vibrations and electronic excitations has been long-standing in surface science.

We recently reported that Br atoms spontaneously desorb from Br-saturated Si(100)-(2×1) in the temperature range 610–775 K.¹² The desorption occurs despite strong Br chemisorption to the surface (~ 3.8 eV) and the fact that known reactions leading to SiBr₂ desorption occur at a much higher temperature (~ 950 K).¹³ We demonstrated that the activation energy and prefactor for the desorption deduced from Arrhenius plots of rates versus inverse temperature depended strongly on the doping of the substrate. Significantly, shifts in the Fermi level position induced by sample doping were accompanied by changes in the activation energy. Thus, desorption resulted from phonon activation of electrons into long-lived Si-Br antibonding states with subsequent desorp-

tion of Br. By analyzing the dependence of the prefactors on the activation energy, we showed that the optical phonons of the Si lattice served as the energy source for the initial excitation.

Using scanning tunneling microscopy, we deduce the temperature-dependent desorption rates as a function of halogen type, doping type, and doping concentration. In this paper, we focus on desorption from Cl- and I-saturated Si(100)-(2×1) at temperatures ranging from 675 to 800 K. This extension beyond a single adsorbate-surface system demonstrates the generality of phonon-activated electron-stimulated desorption (PAESD), and it provides a more detailed understanding of the parameters associated with the process. We show that Cl desorption belongs to the same family of processes that are responsible for Br loss, we calculate the entropy changes associated with the multiphonon nature of the reactions, and we explain how this entropy plays a critical role in the desorption rates. Surprisingly, the rate of desorption for I is nearly three orders of magnitude higher and, to account for it, we propose that conduction-band electrons impinging the surface with the appropriate energy can be captured by the Si-I antibonding states which overlap the conduction-band minimum (CBM). Thus, the rate constant depends on the equilibrium number of carriers with energies corresponding to the CBM, resulting in greater desorption rates.

II. EXPERIMENTAL CONSIDERATIONS

The experiments were carried out in a ultrahigh-vacuum system with a base pressure of 4×10^{-11} Torr. The Si wafers were *p* type (B doped, $\sim 0.010 \Omega \text{ cm}$ corresponding to 7

$\times 10^{18} \text{ cm}^{-3}$, denoted *p*-Si) and *n*-type (P doped, $\sim 0.5 \Omega \text{ cm}$, $9 \times 10^{15} \text{ cm}^{-3}$, denoted *ldn*-Si for lightly doped *n*-Si, and $\sim 0.005 \Omega \text{ cm}$, $1 \times 10^{19} \text{ cm}^{-3}$, denoted *hdn*-Si for heavily doped *n*-Si). Clean surfaces were prepared using thermal treatments¹⁴ and imaged with a scanning tunneling microscope to verify surface quality. They were then exposed to a flux of Cl_2 , Br_2 , or I_2 to achieve surface saturation, defined as one halogen atom bonded to each dangling bond of the (2×1) surface. Thereafter, they were heated to a specific temperature in the range 620–800 K for a specific time in the range 1–90 min, cooled rapidly, and imaged at room temperature.¹⁵ The amount of halogen lost was determined from the number of bare sites per unit area.¹⁶ The imaging conditions had no effect on the halogen concentration, as concluded from repetitive same-area scanning.

III. RESULTS AND DISCUSSION

A. Cl- and Br-Si(100)

Figure 1(a) is representative of Si(100)- (2×1) that has been saturated with Cl. The dimer rows run diagonally across the image, and they are bright and are separated by dark lines. A dimer vacancy (DV) appears as a dark feature that spans the dimer row. The signature of a halogen free or bare dimer (BD) is a symmetric triplet derived from the BD and two bright, halogen-terminated dimers on either side. These triplets reflect the coupling of localized states of the BD with adjacent Si-halogen levels, and their appearance varies with imaging conditions.¹⁶ Figure 1(b) shows the surface of Fig. 1(a) after 20 min at 750 K. We observe the appearance of BD's but no increase in the number of DV's, indicating that halogen desorption is the only reaction that has occurred during the heating period. From results like those of Fig. 1, we can determine the number of desorbed halogen adatoms.

Experiments for Cl, Br, and I like those leading to Fig. 1 were done on *p*-Si at multiple temperatures, and the Br de-

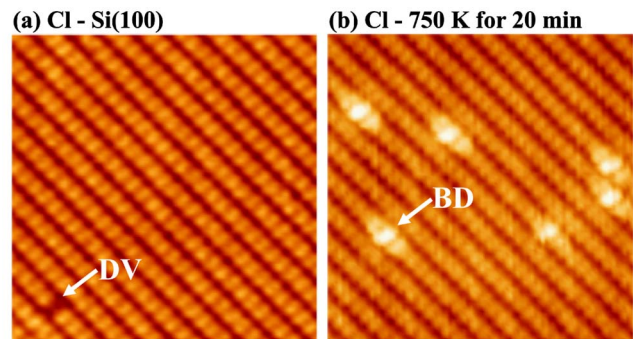


FIG. 1. (Color online) Filled-state scanning tunneling micrographs ($100 \times 100 \text{ \AA}^2$) of Cl on *p*-type Si(100)- (2×1) acquired at room temperature with a sample bias of -1.1 and -1.0 V for (a) and (b), respectively. Dimer vacancies (DV's) appear in each image as dark dimer-sized features. The bare dimers (BD's) appear as bright features involving three dimers, and the middle dimer appears significantly brighter than the two dimers on either side. (a) The initial Cl coverage was 0.999 ML. (b) The sample was heated to the temperature indicated for the time given. The final Cl coverage was 0.989 ± 0.003 ML, giving an average desorption rate of $8.4 \times 10^{-6} \text{ ML s}^{-1}$.

sorption was also studied on *hdn*- and *ldn*-Si samples. As discussed previously,¹² experiments at low temperature were consistent with atomic desorption and diffusing single vacancies that pair up into an energetically favored BD configuration.¹⁷ First-order Arrhenius plots revealed that the activation energies were much lower than the Si-halogen bond strengths of $\sim 4 \text{ eV}$ (Ref. 18) and that the prefactors were much smaller than a typical thermal attempt frequency of $\sim 10^{13} \text{ s}^{-1}$. This indicates that desorption is not simply thermally activated Si-halogen bond breaking. We derive in the Appendix expressions for the activation energy and prefactor for PAESD.

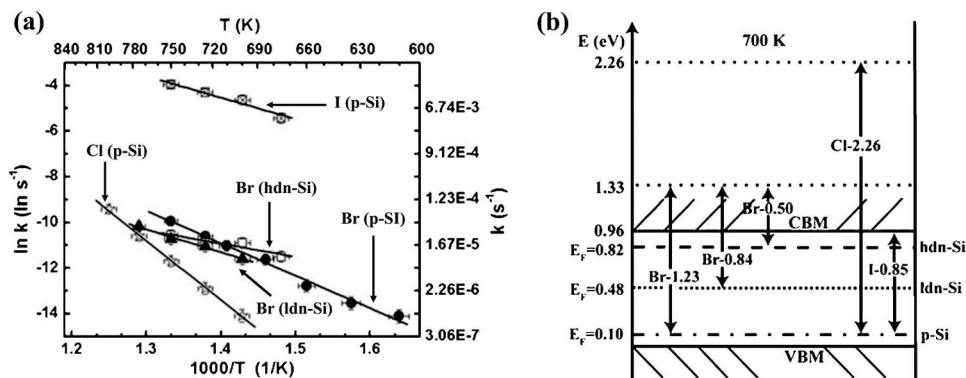


FIG. 2. (a) Arrhenius plots for the desorption of Cl, Br, and I from *p*-Si and for Br from lightly and heavily doped *n*-Si (labeled *ldn*- and *hdn*-Si), from which the kinetic parameters were determined. For Cl and Br, there are rate crossings at 700–800 K and the existence of a common point is possible within experimental uncertainty. For I, the observed rates are nearly three orders of magnitude larger than for Cl and Br. (b) Energy level picture for Si at 700 K. The Fermi levels are indicated by dashed lines, and the energy zero is the valence-band maximum (VBM). The double-headed arrows illustrate the activation energies deduced from experiment, (a). For Br, there is excellent agreement between the shifts in the Fermi levels and the relative changes in the activation energies. The activation energy for Cl desorption is greater than that for Br since the Si-Cl antibonding state lies further from the Fermi level due to the stronger Si-Cl bonding. The activation energy for I corresponds to the energy difference between the CBM and Fermi levels as the Si-I antibonding states overlap the CBM. Electron capture in the σ^* states occurs for all samples, but a shift in the Fermi level changes the internal energy of the reaction.

TABLE I. Thermodynamic properties of the desorption reactions, excited by the optical phonons of Si. The activation energies and prefactors were found from the Arrhenius plots of Fig. 2(a). The phonon entropy is calculated from $\Delta S_{ph}/k_B = \Delta E/\Delta_0$. The number of required phonons is found from $n = \Delta E/(62 \text{ meV})$, where we take the typical energy of the optical phonons to correspond to the peak in the phonon density of states, 62 meV.

Halogen (substrate)	Activation energy ΔE (eV)	Prefactor ν (s^{-1})	Phonon entropy $\Delta S_{ph}/k_B$	Number of required phonons, n
Cl (<i>p</i> -type)	2.26 ± 0.08	$1 \times 10^{10.0 \pm 1.0}$	34	37
Br (<i>p</i> -type)	1.23 ± 0.08	$10^{4.0 \pm 0.5}$	19	20
Br (<i>ldn</i> -type)	0.84 ± 0.09	$10^{1.0 \pm 0.5}$	13	14
Br (<i>hdn</i> -type)	0.50 ± 0.11	$6 \times 10^{-2.0 \pm 0.9}$	8	8
I (<i>p</i> -type)	0.85 ± 0.07	$5 \times 10^{3.0 \pm 1.0}$		

Figure 2(a) shows Arrhenius plots deduced for Cl, Br, and I using Eq. (A5). The activation energies and prefactors determined from straight-line fits are given in Table I. The desorption rates are nearly the same for Cl and Br in the range 700–800 K, but the rate for I is nearly three orders of magnitude larger. In this section, we focus on Cl and Br.

Figure 2(b) shows a schematic band diagram for Si(100) with the relevant energy levels at 700 K. It does not include the entropy components associated with excitation of an electron into the σ^* levels, and the bands are drawn flat since halogen adsorption eliminates the surface states in the gap.^{19–21} Of course, the potential landscape of the surface is much more complicated than the simple one-dimensional model reveals. However, we believe the flatband picture provides a good estimate of the overall surface because of the high density of dopant atoms and the low density of dangling bond states for a saturated surface.^{22,23}

The question arises as to whether the flatband picture continues to be correct after halogen desorption creates dangling bonds. These dangling bonds quickly diffuse to form BD's at the desorption temperatures. On the clean surface, they form a π bond where the π states overlap the valence band and the π^* states lie just below the conduction-band minimum. Only *hdn*-Si could be affected by the position of the π^* states. The surfaces we have studied always maintain a high concentration of Cl and Br during the experiments [>0.94 monolayer (ML)], and we speculate that interactions between the dangling bonds of a BD and the surrounding electronegative halogens shift the π^* states from their clean surface position out of the gap so that the flatband picture remains correct.

The double-headed arrows in Fig. 2(b) show the excitation energies for Cl, Br, and I desorption from the three types of samples. As shown, the Fermi level is about 0.10 eV above the VBM for *p*-Si, 0.48 eV above the VBM for *ldn*-Si, and 0.82 eV above the VBM for *hdn*-Si at 700 K, assuming nondegenerate doping. Significantly, these Fermi-level shifts associated with doping are in excellent agreement with the changes in the activation energies for Br desorption. This implies that in all three cases the electrons are being

excited into the same state which we have proposed to be the Si-Br σ^* state.¹²

Table I shows that the prefactors found from the Arrhenius plots of Fig. 2(a) vary over many orders of magnitude as the activation energies increase from Br on *hdn*-Si to Cl on *p*-Si. The observation that an increase in activation energy is accompanied by an exponential increase in the prefactor is well known from the literature of biological, chemical, and physical processes as the compensation effect or Meyer-Neldel (MN) rule.^{24–27} Quantitatively, the MN rule relates the prefactor and activation energy for a family of processes through $\ln \nu = a + b\varepsilon$ where a and b are constants. Yelon and Movaghar (YM) developed a microscopic model to explain the MN rule, and they showed that the inverse of the slope, $\Delta_0 = 1/b$, is a characteristic energy that provides an order-of-magnitude estimate of the elementary excitations.^{28,29} For Br-Si(100), the best fit to the MN plot ($\ln \nu$ vs ε) gives $\Delta_0 = 60 \pm 5$ meV, implicating optical phonons of the Si lattice as the energy bath.³⁰

Figure 3 shows a MN plot based on the results of Fig. 2(a). The datum point for Cl-*p*-Si increases the energy and the prefactor scales substantially, but the relationship established for Br is continued for Cl with an overall best fit of $\Delta_0 = 66 \pm 5$ meV. The iodine datum point lies off the line, and

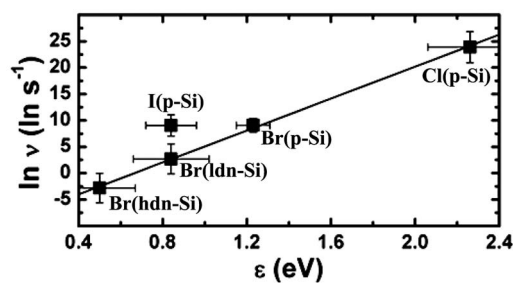


FIG. 3. A MN plot showing that the parameters for Cl match well with those of Br, but that the I datum point does not fall on the line. The inverse of the slope, Δ_0 , is 66 ± 5 meV, and this characteristic energy indicates coupling to the optical phonons of Si.

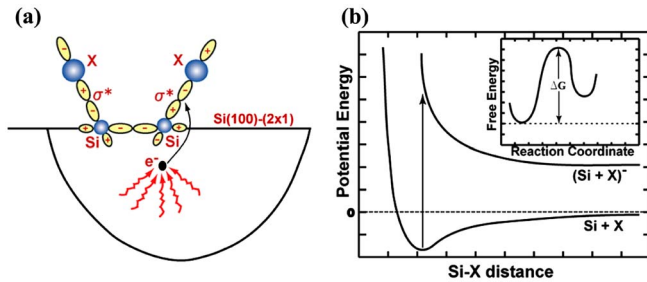


FIG. 4. (Color online) (a) A schematic of multiphonon excitation of an electron into a σ^* state from within an interaction volume around the Si-halogen bond. The excitation rate includes an entropy term that describes the number of ways that phonons can assemble to provide the needed energy. This entropy compensates the change in $(E_{\sigma^*} - E_F)$ caused by doping or by a change in the halogen. (b) A schematic of the potential energy diagram for a system undergoing a Franck-Condon transition from one state to a higher-energy state that is repulsive and which can drive the desorption of the halogen. The inset shows a schematic of the free-energy barrier for desorption. The activated state at the top of the barrier is described by the multiphonon excitation of an electron into the σ^* state. This places the Si-halogen molecule on the repulsive portion of a higher-potential-energy surface and, if the excited state lives long enough, the halogen atom can gain enough kinetic energy to desorb.

it will be discussed in the next section. According to the YM model, to have the activation energies lie on the same MN line means that the reactions belong to the same family of processes. A “family of processes” is defined by having the same energy bath and coupling to that bath. The fact that the Cl and Br data fall in line shows that the phonon spectrum and the electron-phonon coupling are similar for Br and Cl, as would be expected due to the similarity of the Si-halogen bonds. This implicitly assumes that the probability for desorption after excitation, P , is the same for Cl and Br. We speculate that the excited-state lifetimes must be long enough to give $P \sim 1$, rendering differences in masses and potential energy curves irrelevant. If this were not the case, then we are left with the unlikely scenario that differences in escape probability exactly cancel the entropy differences between dissimilar mechanisms governing Cl and Br desorption. We also note that the activation energy for Cl is 1 eV larger than that for Br, consistent with the stronger binding of Cl which should result in a larger separation between the antibonding states of Si-Cl and the Fermi level. We conclude that Cl desorption occurs via PAESD.

The plots for Cl and Br in Fig. 2(a) have crossings between 700 and 800 K, and a common crossing point is within experimental uncertainty. The temperature at which the reaction rates are equal is known as the isokinetic temperature T_{iso} . From the MN rule, T_{iso} is given by Δ_0/k_B which is 767 K from the best fit of Fig. 3. From extrapolation of the plots in Fig. 2(a), the desorption rate is highest for Cl above ~ 800 K even though Cl desorption has, by far, the largest activation energy. Although this result may seem quite surprising at first, it is nicely explained by the YM model.

The YM model demonstrates the crucial role of entropy associated with a reaction whose activation energy is large

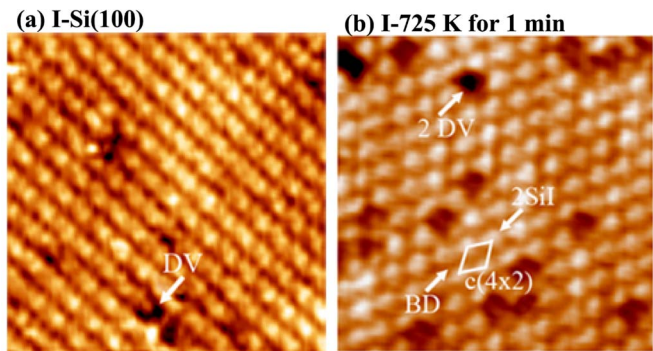


FIG. 5. (Color online) Filled-state scanning tunneling micrographs ($100 \times 100 \text{ \AA}^2$) of I on *p*-type Si(100) acquired with a sample bias of -1.3 and -2.0 V for (a) and (b), respectively. (a) The initial I coverage was 0.999 ML. (b) After heating the initially passivated surface at 725 K for 1 min. Most of the surface exhibits a $c(4 \times 2)$ pattern with dimers that are I terminated appearing as bright features and those that are I free as the dark features that alternate with the bright features. The final coverage was 0.44 ML, giving an average desorption rate of $9.3 \times 10^{-3} \text{ ML s}^{-1}$.

compared to $k_B T$ and the elementary excitations of the system—e.g., phonons. A reaction satisfying the previous condition requires multiple phonons to reach the activated state, and there is a large change in entropy resulting from the number of ways the phonons can be assembled. This entropy is included in the prefactor, as can be seen in Eq. (A4), and Peacock-Lopez and Suhl and later YM showed that it is directly proportional to the enthalpy of activation.^{29,31} Therefore, an increase in the activation energy will result in an exponential increase of the prefactor, naturally giving rise to the compensation effect.

Table I summarizes several properties related to multiphonon electron excitation processes for Cl and Br on Si surfaces with different doping types and concentrations. The activation energies and prefactors were found from the fits to the Arrhenius plots of Fig. 2(a). The phonon entropy is calculated from Eq. (A7) (see the Appendix), and the average number of required phonons is $n = \Delta E / (62 \text{ meV})$ where we take the typical phonon energy to be equal to the peak in the phonon density of states for Si, 62 meV.³²

The phonon entropy given in Table I is the key idea behind the YM model, and it is critical in determining the reaction rate. As shown, the larger activation energy for Cl-*p*-Si requires more phonons and, thus, the reaction has the larger entropy. This entropy competes with the activation energy to determine the rate of the reaction. Below the isokinetic temperature, the reaction with the largest activation energy has the lowest rate, as expected. Above the isokinetic temperature, the entropy “wins” and the reaction with the largest activation energy has the highest rate. It is important to note that the reaction with the highest activation energy has the lowest free-energy barrier above the isokinetic temperature due to the phonon entropy. As discussed by Young and Crandall,³³ the entropy term given by ΔS_{other} must be negative to prevent ΔG from approaching zero as the isokinetic temperature is reached.

The compensation effect cannot continue indefinitely for larger and larger activation energies. The energy for the ex-

citation is supplied from a volume in which an effective coupling exists between the system and surrounding energy and particle reservoir. This interaction volume for a family of processes plays the important role of limiting the range of activation energies for which the compensation effect occurs. Consider a family of processes in which there are N phonons available in the interaction volume. We presume that the statistical distribution describing the entropy, ΔS_{pho} , is well approximated by an exponential distribution only when the required number of phonons, n , is much less than N . For the range of activation energies in which this is true, the compensation effect is obtained. However, for increasingly large activation energies, n approaches N and the distribution describing the entropy deviates substantially from the exponential form and at some point reverses sign. Physically, this behavior must take place because otherwise reactions with unrealistically large activation energies would occur.

Figure 4 is a schematic that summarizes phonon-activated electron-stimulated desorption. In Fig. 4(a), the wavy lines represent multiple optical phonons combining to excite an internal electron into the Si-halogen antibonding state. This excitation occurs within an interaction volume around the Si-halogen "molecule," and it is represented schematically in Fig. 4(b). The capture of the electron in the Si-halogen antibonding state moves the Si-halogen molecule to a new potential energy surface. The inset shows a typical reaction barrier where ΔG is the change in Gibbs free energy between the ground state and the activated state. Here, the activated state is reached when electron capture occurs. The activated molecule finds itself on the repulsive portion of a new potential energy surface so that Cl or Br move away from the silicon. For desorption to occur, the excited state must live long enough for the adatom to acquire sufficient kinetic energy.³⁴

There are several possibilities for the evolution of the excited state during the desorption event, and the process must conserve energy while breaking a 3–4-eV bond. The electron captured in the antibonding state can be transferred to the halogen atom, leading to the desorption of a negative ion, or the electron can be transferred back to the Si, resulting in neutral atom desorption. A rough estimate of the energy required to desorb a negative ion is given by the difference between the electron affinity of the halogen atom and the work function of halogen-terminated Si(100). This gives a value of 1 eV if we assume the work function is close to 4.5 eV and the electron affinity of the halogens is about 3.5 eV. Therefore, the energy gained from the electron transition would be enough to desorb the ion. However, if the electron is transferred back to the silicon during the desorption event, the energy gained from the electron transition is not enough. Either the electron transitions back into a deep hole state or the remaining energy must come from phonons. We speculate that the phonons serve to weaken the Si-Br bond as well as provide the energy for the electronic excitation to the Si-Br antibonding state.

B. I-Si(100)

Figure 5 shows an I-Si(100) surface after only 1 min at 725 K. The surface was initially saturated with I. The dimers

with I appear bright, the bare dimers appear darker, and the DV's again appear as dark spots that are the full width of the dimer row. The I is arranged in a $c(4 \times 2)$ pattern that arises due to strong steric repulsive interaction between the large adatoms.^{35,36} Analysis reveals the initial and final coverages were 0.999 ML and 0.44 ML. The average desorption rate is then 9.3×10^{-3} ML s^{-1} , which is nearly three orders of magnitude larger than for Cl and Br desorption at this temperature. From Fig. 2(a), the best fit to the I data gives an activation energy of 0.85 eV with a prefactor of $5 \times 10^3 s^{-1}$. Although the activation energy could be consistent with electron capture in the Si-I antibonding states, Fig. 3 shows that I does not fit on the curve for the PAESD processes of Cl and Br. Either one of the terms in the prefactor is significantly altered for I or a new mechanism dominates the desorption.

From Eq. (A4), an increase in the prefactor must arise from an increase in P , the probability of desorption after excitation. In principle, the increase in the desorption rate could reflect a much-increased lifetime of the Si-I σ^* state. Although we have no way to test this possibility, we think it is unlikely due to the chemical similarity of the halogen bonds. Although the large steric repulsive energies involving the iodine adatoms^{35,36} could alter the shapes and relative positions of the potential curves of Fig. 4(b), they do not account for the increased rate. This conclusion is based on a desorption experiment where the initial I coverage was ~ 0.42 ML and steric repulsive interactions would be greatly reduced.³⁷ After 1 min at 725 K, the coverage decreased to 0.22 ML. The corresponding rate fits in the first-order Arrhenius plot of Fig. 2(a), within experimental error, without any indication that steric interactions significantly influence the rate of desorption.

Although the PAESD reaction would still occur for I-Si(100), it is apparently not the dominant mechanism driving the I desorption. We propose a second contribution that involves the capture of free carriers by the Si-I σ^* states. Due to the relatively weaker bonding of I, the σ - σ^* separation is smaller than for Cl or Br and the Si-I σ^* states overlap with the CBM. Since there are a large number of free carriers within $k_B T$ of the CBM, free carriers that reach the surface can be captured by the Si-I σ^* states. This process is similar to PAESD in that both involve the localization of an electron in the antibonding states, but they are distinguishable.

PAESD involves the rare process of many phonons combining to excite an electron directly into the σ^* state while desorption induced by the capture of free carriers is governed by the equilibrium number of electrons at the CBM impinging on the surface. The capture of free carriers does not involve the large entropy change associated with the assembly of multiple phonons, ΔS_{pho} . Hence, the capture of free carriers can be ruled out for Cl and Br since rate crossings are observed that can only be explained by the multiphonon entropy term in the rate equation. The iodine desorption datum point does not lie on the Br and Cl lines of the Meyer-Neldel plot in Fig. 3 since any multiphonon excitation of electrons into the σ^* states is overwhelmed by direct electron capture. The data still fit a first-order Arrhenius plot since the equilibrium number of electrons at the CBM is well described by Boltzmann statistics. Significantly, the activation energy of 0.85 eV matches well the energy separation be-

tween E_F and the CBM at the elevated temperatures for p -Si. Thus, the much more frequent occurrence of free-electron capture results in a huge increase in the prefactor and, thus, in the desorption rate.

IV. CONCLUSIONS

The results presented here demonstrate that the desorption of halogens from Si(100) results from complex processes involving both phonons and electronic excitations. Moreover, large entropy changes are critical components of the reactions and, for Cl and Br, they lead to crossovers in the desorption rates. For the halogen-Si system, this desorption pathway is important because the halogen coverage is a key parameter in etching and roughening reactions, in surface patterning, and in equilibrium morphologies. The results point to charge carriers playing a more general role in surface reactions than has been previously recognized.

ACKNOWLEDGMENTS

We thank R.S. Crandall and A.M. Wodtke for stimulating discussions. This work was supported by the National Science Foundation. V.N.A. was supported by the Department of Energy under Award No. DEFG02-91-ER45439 through the Frederick Seitz Materials Research Laboratory at the University of Illinois.

APPENDIX

The following analysis shows that Eq. (A4) provides accurate values for the activation energy and prefactor. The general expression for a first-order reaction rate is

$$r = -\frac{d\theta}{dt} = k\theta \quad (\text{A1})$$

where k is the rate constant, θ is the reactant (halogen) concentration, and t is time. For PAESD involving electron localization in the Si-halogen antibonding level at energy E_{σ^*} , the rate constant is $k=IP$ where I is the electron capture rate in units of s^{-1} . Capture introduces one extra electron and results in an activated state that resides on a new potential energy surface via a Franck-Condon transition. P is the probability that this state will lead to halogen desorption. The rate of transition to the activated state is described by Eyring theory³⁸ as

$$I = A \exp\left(\frac{-\Delta G}{k_B T}\right), \quad (\text{A2})$$

where A is a constant and $\Delta G = \Delta H - T\Delta S$ is the difference in the Gibbs free energy between the ground state and the excited state with an electron in σ^* . Treating the Si-halogen molecule as a two-state system in equilibrium with an energy and particle reservoir, we can split the change in entropy, ΔS , into three parts—one associated with adding an electron to the σ^* state, ΔS_e ; one associated with the phonons involved in the excitation process, ΔS_{pho} , to be discussed below; and one associated with any other changes in the molecular reaction, ΔS_{other} , presumed to be the same for each sample. ΔS_e is related to the chemical potential μ through the ther-

modynamic relation $\mu = -T \Delta S_e / \Delta N$, where $\Delta N = -1$ is the change in the number of electrons. Also, the enthalpy $\Delta H \approx \Delta E = E_{\sigma^*}$ where we have defined $E = 0$ for the ground state. Thus, the capture rate can be written

$$I = A \exp\left(\frac{\Delta S_{pho} + \Delta S_{other}}{k_B}\right) \exp\left(-\frac{E_{\sigma^*} - \mu}{k_B T}\right), \quad (\text{A3})$$

where $\mu = E_F$. The rate constant is then

$$k = \nu \exp\left(-\frac{\varepsilon}{k_B T}\right), \quad (\text{A4})$$

where

$$\nu = PA \exp\left(\frac{\Delta S_{pho} + \Delta S_{other}}{k_B}\right)$$

is the prefactor and $\varepsilon = |E_{\sigma^*} - E_F| \gg k_B T$ is the activation energy. Substituting Eq. (A4) into Eq. (A1) gives

$$\ln k = \ln \left[\frac{1}{t} \ln \left(\frac{\theta_i}{\theta_f} \right) \right] = -\frac{\varepsilon}{k_B T} + \ln \nu. \quad (\text{A5})$$

Equation (A5) is important because θ_i , θ_f , and t are known in each experiment. Note that Eqs. (A4) and (A5) are very general Arrhenius expressions that would fit most first-order reactions and specific assignment of the kinetic parameters is only meaningful in light of a specific reaction mechanism. The activation energy of Eq. (A4) is taken as the energy separation between the Si-halogen antibonding states and the Fermi level. However, this separation depends on temperature since both the Fermi level and the gap have temperature dependences. Also, the entropy factor is temperature dependent because Peacock-Lopez and Suhl and later YM showed that the phonon entropy is directly proportional to the activation enthalpy.^{29,31} Though the shifts in the Fermi level and band gap are small in the temperature range studied, we must determine if their temperature dependences lead to apparent kinetic parameters that are larger or smaller than the actual parameters.

To test this, we explicitly substitute the known temperature dependencies of E_F and the band gap into Eq. (A4) and use the resulting equation to fit a plot of $\ln k$ vs T . We will use p -Si as an example but note that the cases of ldn - and hdn -Si are similar. We assume that the Si-halogen antibonding states are fixed with respect to the CBM—i.e., that the σ - σ^* separation has the same temperature dependence as the band edges so that σ^* moves with the CBM. It is convenient to define the CBM to have $E = 0$. We write Eq. (A4) as

$$k = PA \exp\left(\frac{\Delta S_{other}}{k_B}\right) \exp\left(\frac{\Delta S_{ph}}{k_B}\right) \exp\left(-\frac{E_{\sigma^*} - E_F}{k_B T}\right). \quad (\text{A6})$$

From the MN rule, we can write the phonon entropy as

$$\Delta S_{ph} = k_B b (E_{\sigma^*} - E_F), \quad (\text{A7})$$

where b is the slope of the best fit in Fig. 3 and we have assumed that ΔS_{other} is not directly proportional to ΔE . We also use the temperature-dependent expressions for E_F (Ref. 39) and the band gap⁴⁰

$$E_F = -E_g + k_B T \ln\left(\frac{N_V}{N}\right), \quad (\text{A8a})$$

$$E_g(T) = E_g(0) - \frac{\alpha T^2}{T + \beta}, \quad (\text{A8b})$$

where N_V is the density of states in the valence band, N_A is the dopant concentration, $E_g(T)$ is the band gap energy at temperature T , $E_g(0)$ is the band gap energy at 0 K, and α and β are constants. We have ignored the temperature dependence of N_V since it is inside the logarithm. Substituting Eqs. (A6)–(A8) into Eq. (A5) gives

$$\begin{aligned} \ln k &= \ln \left[\frac{1}{t} \ln \left(\frac{\theta_i}{\theta_f} \right) \right] \\ &= \ln \nu_0 + \left(b - \frac{1}{k_B T} \right) E_{\sigma^*} - \frac{E_g(0)}{k_B T} - b k_B T \ln \left(\frac{N_V}{N_A} \right) \\ &\quad - \frac{b \alpha T^2}{T + \beta} + \frac{\alpha T}{k_B T + k_B \beta} + b E_g(0) + \ln \left(\frac{N_V}{N_A} \right), \quad (\text{A9}) \end{aligned}$$

where $\nu_0 = AP \exp(\Delta S_{\text{other}}/k_B)$. We emphasize that E_{σ^*} is measured with respect to the CBM.

Fitting a plot of $\ln k$ vs T with Eq. (A9) gives $E_{\sigma^*} = 1.45 \pm 0.18$ eV with $\nu_0 = 3 \times 10^{-5.0 \pm 0.1} \text{ s}^{-1}$ and $E_{\sigma^*} = 0.31 \pm 0.06$ eV with $\nu_0 = 7 \times 10^{-5.0 \pm 0.1} \text{ s}^{-1}$ for Cl and Br desorption, respectively. Note from the small values of ν_0 that either P must be a very small number or ΔS_{other} must be a large negative number, or both. To compare these values to those found using Eq. (A4), we must add to the activation energies the energy separation of 0.86 eV between the CBM and E_F , and we must multiply the prefactors by the exponential of the phonon entropy. This gives 2.31 eV with $1.8 \times 10^{10} \text{ s}^{-1}$ and 1.17 eV with $1.2 \times 10^4 \text{ s}^{-1}$, very close to the values found from Fig. 2(a). A similar analysis for *ldn*- and *hdn*-Si also gave values that closely matched those found from the Arrhenius plots of Fig. 2(a). We conclude that the temperature dependences of the Fermi level and band gap in Eq. (A4) do not lead to significant errors in the kinetic parameters.

*Current address: Micron Technology, Inc., Mail Stop 1–719, 8000 S. Federal Way, Boise, ID 83707–0006.

†Current address: GE Advanced Materials, Quartz, 24400 Highland Road, Richmond Heights, OH 44143, USA.

‡Current Address: Institute for Materials Research, Tohoku University, Sendai 980-8577, Japan.

¹R. D. Ramsier and J. T. Yates, Jr., *Surf. Sci. Rep.* **12**, 243 (1991).

²T. E. Madey, *Surf. Sci.* **299/300**, 824 (1994).

³T.-C. Shen, C. Wang, G. C. Abeln, J. R. Tucker, J. W. Lyding, Ph. Avouris, and R. E. Walkup, *Science* **268**, 1590 (1995).

⁴E. T. Foley, A. F. Kam, and J. W. Lyding, and Ph. Avouris, *Phys. Rev. Lett.* **80**, 1336 (1998).

⁵K. Mochiji and M. Ichikawa, *Phys. Rev. B* **63**, 115407 (2001).

⁶J. Kanasaki, M. Nakamura, K. Ishikawa, and K. Tanimura, *Phys. Rev. Lett.* **89**, 257601 (2002).

⁷K. Nakayama and J. H. Weaver, *Phys. Rev. Lett.* **82**, 980 (1999).

⁸B. S. Swartzentruber, *Phys. Rev. Lett.* **76**, 459 (1996).

⁹E. Hill, B. Freelon, and E. Ganz, *Phys. Rev. B* **60**, 15896 (1999).

¹⁰M. Dürr, A. Biedermann, Z. Hu, U. Höfer, and T. F. Heinz, *Science* **296**, 1838 (2002).

¹¹C. M. Aldao and J. H. Weaver, *Prog. Surf. Sci.* **68**, 189 (2001).

¹²B. R. Trenhaile, V. N. Antonov, G. J. Xu, Koji S. Nakayama, and J. H. Weaver, *Surf. Sci. Lett.* **583**, L135 (2005).

¹³M. C. Flowers, N. B. H. Jonathan, Y. Liu, and A. Morris, *Surf. Sci.* **343**, 133 (1995).

¹⁴K. Hata, T. Kimura, S. Ozawa, and H. Shigekawa, *J. Vac. Sci. Technol. A* **18**, 1933 (2000).

¹⁵The temperature was monitored with an optical pyrometer calibrated with a W-Re thermocouple; heating rate $\sim 3 \text{ K s}^{-1}$; reproducibility $\pm 5 \text{ K}$.

¹⁶G. J. Xu, E. Graugnard, B. R. Trenhaile, Koji S. Nakayama, and J. H. Weaver, *Phys. Rev. B* **68**, 075301 (2003). For Cl-Si(100) at a sample bias of -0.8 V , the BD appears much brighter than the two dimers on either side, while for Br-Si(100) at a sample

bias of -0.6 V , the two dimers on either side appear brighter than the BD.

¹⁷G. A. de Wijs, A. De Vita, and A. Selloni, *Phys. Rev. B* **57**, 10021 (1998).

¹⁸*CRC Handbook of Chemistry and Physics*, 75th ed., edited by D. R. Lide (CRC Press, Boca Raton, 1995).

¹⁹R. J. Hamers, Ph. Avouris, and F. Bozso, *Phys. Rev. Lett.* **59**, 2071 (1987).

²⁰L. Liu, J. Yu, and J. W. Lyding, *Appl. Phys. Lett.* **78**, 386 (2001).

²¹A. W. Signor, K. S. Nakayama, and J. H. Weaver (unpublished).

²²S. Roy and A. Asenov, *Science* **309**, 388 (2005).

²³P. G. Piva, G. A. DiLabio, J. L. Pitters, J. Zikovskiy, M. Rezeq, S. Dogel, W. A. Hofer, and R. A. Wolkow, *Nature (London)* **435**, 658 (2005).

²⁴W. Meyer and H. Neldel, *Z. Tech. Phys. (Leipzig)* **12**, 588 (1937).

²⁵A. K. Galwey, *Adv. Catal.* **26**, 247 (1977).

²⁶B. Rosenberg, G. Kemeny, R. C. Switzer, and T. C. Hamilton, *Nature (London)* **232**, 471 (1971).

²⁷R. S. Crandall, *Phys. Rev. B* **66**, 195210 (2002).

²⁸A. Yelon and B. Movaghar, *Phys. Rev. Lett.* **65**, 618 (1990).

²⁹A. Yelon, B. Movaghar, and H. M. Branz, *Phys. Rev. B* **46**, 12244 (1992).

³⁰Yelon *et al.*, in Ref. 29 fitted data for deep trapping in crystalline silicon and found a Δ_0 value of $50 \pm 25 \text{ meV}$. They also showed that values of Δ_0 in the range of $35\text{--}70 \text{ meV}$ are plausible for coupling to optical phonons for semiconductors with band gaps of $1\text{--}2 \text{ eV}$.

³¹E. Peacock-Lopez and H. Suhl, *Phys. Rev. B* **26**, 3774 (1982).

³²M. P. Marder, *Condensed Matter Physics* (Wiley, New York, 2000), p. 320.

³³D. L. Young and R. S. Crandall, *Appl. Phys. Lett.* **86**, 262107 (2005).

³⁴Koji S. Nakayama, E. Graugnard, and J. H. Weaver, *Phys. Rev.*

- Let. **89**, 266106 (2002), showed that electron capture in the Si-Br antibonding state was sufficiently long lived to induce Br hopping. A detailed calculation of the lifetimes is beyond the scope of this paper.
- ³⁵G. J. Xu, N. A. Zarkevich, Abhishek Agrawal, A. W. Signor, B. R. Trenhaile, D. D. Johnson, and J. H. Weaver, *Phys. Rev. B* **71**, 115332 (2005).
- ³⁶Dongxue Chen and John J. Boland, *Phys. Rev. B* **67**, 195328 (2003).
- ³⁷Reference 36 found that the second-nearest-neighbor interaction diagonally across the dimer row was negligible (~ 5 meV) for F1, Cl, and Br. Here, we assume that the trend continues so that the second-nearest-neighbor interaction for I is much less than nearest-neighbor interactions. An experiment of this type with Cl or Br would roughen the surface so much that an accurate measurement of the halogen coverage would not be possible.
- ³⁸S. Glasstone, K. J. Laidler, and H. Eyring, *The Theory of Rate Processes* (McGraw-Hill, New York, 1941).
- ³⁹S. M. Sze, *Physics of Semiconductor Devices*, 2nd ed. (Wiley, New York, 1981), derives in the introduction the expression used for Eq. (A8a). Note that since we have defined $E_{CBM}=0$ we can write $E_{VBM}=-E_g$.
- ⁴⁰J. I. Pankove, *Optical Processes in Semiconductors* (Dover, New York, 1971), p. 27, discussed the temperature dependence of semiconductor band gaps. For silicon, the bulk band gap decreases from 1.00 eV at 620 K to 0.93 eV at 775 K.